Mon. Not. R. Astron. Soc. **000**, 1 (2005) Printed 28 October 2005 (MN LATEX style file v2.2)

A closer look at the X-ray transient XTE J1908+094: identification of two new near-infrared candidate counterparts ⋆

S. Chaty [1], R.P. Mignani [2], G.L. Israel [3]
[1] *AIM - Astrophysique Interactions Multi-échelles (Unité Mixte de Recherche 7158 CEA/CNRS/Université Paris 7 Denis Diderot), CEA Saclay, DSM/DAPNIA/Service d'Astrophysique, Bât. 709, L'Orme des Merisiers, FR-91 191 Gif-sur-Yvette Cedex, France* †
[2] *ESO, Karl Schwarzschild Str. 2, D-85748 Garching bei München, Germany*
[3] *INAF - Osservatorio Astronomico di Roma, Via Frascati 33, I-00040, Monteporzio Catone, Italy*

Received date; Accepted date

ABSTRACT
We had reported in Chaty et al. (2002a) on the near-infrared (NIR) identification of a possible counterpart to the black hole candidate XTE J1908+094 obtained with the ESO/NTT. Here, we present new, follow-up, CFHT adaptive optics observations of the XTE J1908+094 field, which resolved the previously proposed counterpart in two objects separated by about $0\farcs8$. Assuming that both objects are potential candidate counterparts, we derive that the binary system is a low-mass system with a companion star which could be either an intermediate/late type (A-K) main sequence star at a distance of 3-10 kpc, or a late-type (>K) main sequence star at a distance of 1-3 kpc. However, we show that the brighter of the two objects ($J \sim 20.1$, $H \sim 18.7$, $K' \sim 17.8$) is more likely to be the real counterpart of the X-ray source. Its position is more compatible with our astrometric solution, and colours and magnitudes of the other object are not consistent with the lower limit of 3 kpc derived independently from the peak bolometric flux of XTE J1908+094. Further multi-wavelength observations of both candidate counterparts are crucial in order to solve the pending identification.

Key words: stars: individual: XTE J1908+094, X-rays: binaries, optical: stars, infrared: stars

1 INTRODUCTION

The X-ray transient XTE J1908+094 was serendipitously discovered on 2002 February 21 during observations of the field of the Soft Gamma-ray Repeater SGR 1900+14 performed with the Proportional Counter Array (PCA) aboard RXTE (galactic coordinates $l, b = 43.26\,\mathrm{deg}, +0.43\,\mathrm{deg}$; Woods et al. 2002). Within one month after its discovery, the source flux increased by a factor ~ 3 and broad peak QPOs at a frequency of 1 Hz were also detected. The RXTE/PCA 2-30 keV spectrum was found consistent with a power-law (photon index=1.55) with an hydrogen column density $N_H = 2.3 \times 10^{22}$ cm^{-2} (Woods et al. 2002). Soon after, XTE J1908+094 was observed at higher energies ($15 - 300$ keV) with the PDS aboard *BeppoSax* (Feroci & Reboa 2002), at a flux level inconsistent with the extrapolation of the RXTE/PCA power law, implying a cut-off in the X-ray spectrum at energies around 100 keV. Target of Opportunity (ToO) observations performed with the MECS on *BeppoSax* (in 't Zand et al. 2002a) provided a source positioning better than $20''$, while the measurement of the source flux in outburst set a lower limit on the distance of 3 kpc (in't Zand et al. 2002b). The transient radio counterpart to XTE J1908+094 was identified with the Very Large Array (VLA), with a position uncertainty of $0.1''$ in each coordinate (Rupen et al. 2002), consistent with the improved Chandra/ACIS position (in't Zand et al. 2002b). First follow-up optical observations failed to detect any possible counterpart brighter than $R \sim 23$ (Wagner & Starrfield 2002) and $I \sim 22$ (Garnavich et al. 2002). Thereafter, Chaty et al. (2002b) reported the discovery of a likely near-infrared (NIR) counterpart, apparently variable along the X-ray lightcurve (Chaty et al. 2002a).
Here, we report on the results of new, follow-up, adaptive optics NIR observations of the XTE J1908+094 candidate

⋆ Based on observations obtained at the Canada-France-Hawaii Telescope (CFHT) which is operated by the National Research Council of Canada, the Institut National des Science de l'Univers of the Centre National de la Recherche Scientifique of France, and the University of Hawaii.
† chaty@cea.fr

counterpart. The observations are described in Section 2, while the results are discussed in Section 3.

2 OBSERVATIONS AND DATA REDUCTION

The first NIR observations of the XTE J1908+094 field were obtained in April and June 2002 with the SOFI camera at the ESO 3.5m New Technology Telescope (NTT) and are described in Chaty et al. (2002a). New NIR observations were performed on 2002 August 18 in visitor mode with the 3.6m Canada-France-Hawaii Telescope (CHFT) on top of Mauna Kea (Hawaii). The observations were carried out using the Adaptive Optics Bonnette (PUEO), mounted at the f/8 CFHT Cassegrain focus, equipped with the KIR instrument. This is a near-infrared imaging camera based on the 1024×1024 Rockwell Science Center HAWAII (HgCdTe Astronomical Wide Area Infrared Imaging) focal plane array, sensitive to radiation from 0.7 to 2.5 μm. The camera plate scale is $0\farcs035$/pixel, yielding a total field-of-view of $36'' \times 36''$.

Images were taken through the J ($\lambda = 1.250$ μm, $FWHM = 0.160$ μm), H ($\lambda = 1.635$ μm, $FWHM = 0.290$ μm) and K' ($\lambda = 2.120\mu$m, $FWHM = 0.340\mu$m) filters. The source was observed through a sequence of 5 exposures of 90s each in the J, H and K' filters, respectively, with a random offset among images in order to perform background subtraction of the variable IR sky. Conditions were photometric. The airmass was between 1.02 and 1.04, the typical seeing conditions were around $0.4'' - 0.6''$ and the adaptive optics resulted in a source Point Spread Function (PSF) of about $0\farcs1-0\farcs14$ in the images (diffraction limited). The images have been corrected for instrumental effects, by removal of the dark current and flat-fielding, and then sky subtracted, using standard procedures available in the IRAF package *ccdred*. For each filter, we finally computed a final image which is the median of the sequence. Photometric calibration was performed using the standard star field FS35 (G21-15; Casali 1992).

3 RESULTS

3.1 Astrometry

To accurately register the radio coordinates of the source (Rupen et al. 2002) on the CFHT images, we have computed the image astrometry using as a reference the positions of stars selected from the Two Micron All Sky Survey (2MASS) Point Source Catalogue, which has an intrinsic absolute astrometric accuracy of $\sim 0\farcs2$ per coordinate[1]. Due to the smaller field of view of the CFHT camera ($36'' \times 36''$), only 11 2MASS objects have been identified in the averaged J-band image and used as suitable astrometric calibrators. The pixel coordinates of the reference stars have been computed by a two-dimensional gaussian fitting procedure, and transformation from pixel to sky coordinates was then computed using the programme ASTROM[2], yielding an rms of $\sim 0\farcs08$ in both Right Ascension and Declination, which we assume representative of the accuracy of our astrometric solution. After taking into account the rms of the astrometric fit ($\sim 0\farcs08$), the absolute accuracy of the 2MASS coordinates ($\sim 0\farcs2$) and the error of the source radio coordinates ($0\farcs1$, Rupen et al. 2002), we estimated $\sim 0\farcs24$ (per coordinate) to be the final uncertainty on the computed source position.

Figure 1 shows $15'' \times 15''$ and $4\farcs5 \times 4\farcs5$ cutouts of the NTT and CFHT J-band images centered around the computed source position (left and right panel, respectively). In the CFHT image we overplot the 1 and 3 σ error circles derived from our astrometric solution. One and two objects, labelled 1 and 2 in figure 1 (right panel), are found within the 1σ and 3σ error circles, respectively. As the angular separation between objects 1 and 2 is about $0\farcs8$, we note that they could have been hardly resolved in the SOFI images of Chaty et al. (2002a), in view of the non-optimal seeing conditions ($0\farcs8 - 1\farcs2$) during the observations and of the much larger pixel size of the detector ($0\farcs292$). Thus, we conclude that the previously proposed candidate counterpart was actually the blend of these two objects.

Although both objects are considered as potential counterparts in the following analysis, we note that object 1 (the brighter of the two) is certainly favoured as its position is more consistent with our astrometric solution.

3.2 Photometry

We have computed the JHK' photometry of the two candidate counterparts (objects 1 and 2) identified in the CFHT images. In order to obtain more precise measures, we have used the *IRAF/DAOPHOT* package for the photometry in crowded fields. Specifically, we computed a typical PSF for every image using the tasks *daofind, phot, psf, nstar* and *substar*, iterating the procedure to minimize the residuals after PSF subtraction. Then, we ran a star subtraction algorithm through the task *allstar* (Massey & Davis 1992) to remove all objects detected in the neighbourhood of our candidate counterparts before computing their magnitudes. The final CFHT JHK' magnitudes of objects 1 and 2 are reported in rows 4 and 5 of Table 1.

Using the same procedure described above, we have reanalyzed the original NTT images of Chaty et al. (2002a) in an attempt to resolve, or at least constrain, the flux of objects 1 and 2. Unfortunately, the highly uncertain residuals after the PSF subtraction make it impossible to derive reliable magnitude estimates for both objects. Thus, we have taken the magnitudes reported in Chaty et al. (2002a), which correspond to the blend of objects 1 and 2, as upper limits on the actual magnitudes of these two objects. These values are listed in the first three rows of Table 1.

As no direct evaluation of the variability of objects 1 and 2 is possible from the current photometry, we have tried to obtain an indirect piece of evidence by simply comparing the combined flux of the two objects measured in the CFHT images (Table 1, last row) with the flux of the blend measured in the NTT ones (Table 1, first three rows). As it is seen from Table 1, in the H and K bands the combined flux of objects 1 and 2 is significantly fainter than the flux of the blend at the different epochs (it is also true in the J-band, however we point out that the large error attached to the 2002-06-17 measurement hide any variation). In other

[1] http://spider.ipac.caltech.edu/staff/hlm/2mass/overv/overv.html
[2] http://star-www.rl.ac.uk/Software/software.htm

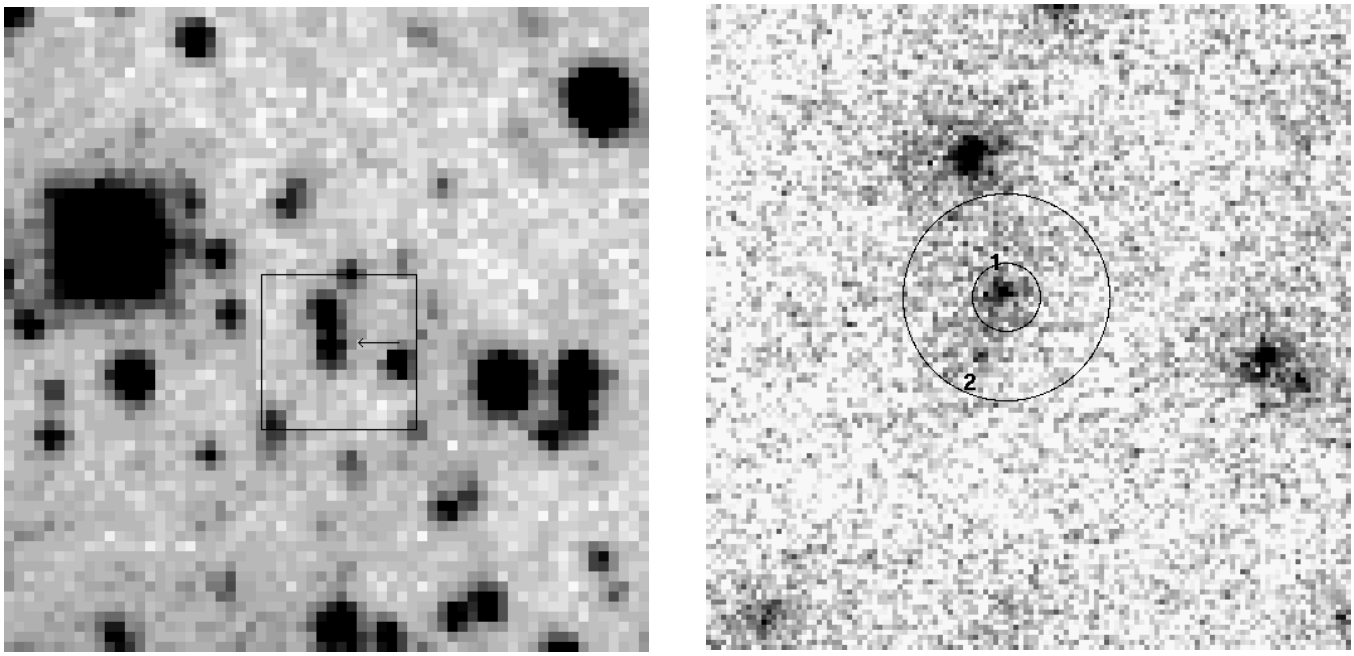

Figure 1. Left panel: $15'' \times 15''$ cutout of the NTT/SOFI J-band image of the XTE J1908+094 field (Chaty et al. 2002a), with the previously suggested candidate counterpart marked by an arrow. North to the top, East to the left. Right panel: $4\farcs5 \times 4\farcs5$ cutout (corresponding to the box in the left panel) of the combined CFHT/KIR J band image of the same field. In the CFHT image, the two circles (of radius $0\farcs24$ and $0\farcs71$, respectively) correspond to the 1σ and 3σ uncertainties on the source position derived from our astrometric solution and the target radio position ($\alpha(J2000) = 19^{\rm h}08^{\rm m}53\overset{\rm s}{.}77 \pm 0\overset{\rm s}{.}007$; $\delta(J2000) = +09^\circ 23' 04\farcs9 \pm 0\farcs1$) from Rupen et al. (2002). The two possible candidate counterparts detected within the 3σ error circle are labelled (1 and 2).

words, the IR flux of one of the two objects (or both) varied in the time span covered by our observations.

To search for a possible correlation between the observed IR and X-ray variability, we have compared our photometry reported in Table 1 with the RXTE/ASM lightcurve of XTE J1908+094 (Figure 2, top panel). First, we considered as before the total JHK magnitudes of objects 1 and 2 (Table 1, last row) and the magnitudes of the blend (Table 1, first three rows). These are plotted in Figure 2 (middle panel). Second, we considered the actual JHK magnitudes of objects 1 and 2 (Table 1, rows 4 and 5) with the expected magnitudes derived from the NTT/SOFI upper limits. As a crude approximation, we have straightly computed (per each passband) the difference between the NTT/SOFI flux of the blend and the CFHT/KIR flux of objects 1 and 2 in turn, assuming the other constant. The resulting lightcurves are shown in Figure 2 (lower panel). From the IR lightcurves it is clear that either object 1 or 2 (or both) have undergone a significant decrease of the NIR flux consistent with the X-ray flux decay which occurred in the time span covered by our observations. This variability means that, almost certainly, one of the two objects is the real counterpart of the X-ray source XTE J1908+094.

3.3 The companion star

We have used our JHK' band photometry to derive constraints on the nature of the two XTE J1908+094's candidate counterparts. For both objects 1 and 2, we have taken the magnitudes measured on August 18th 2002, i.e. likely at the minimum, as inferred from the X-ray lightcurve (Figure 2, upper panel), assuming that all the flux is produced by the companion star. However, we have to caution that this assumption might not be entirely valid, since Figure 2 shows that the X-ray source still exhibited some level of activity at this epoch. Therefore, it is likely that the infrared emission was not produced purely from the companion star but was contaminated by the contribution of the accretion disc. For this reason, we have prudently assumed the derived absolute magnitudes as upper limits on the luminosity of the companion star.

We show in Figure 3 a theoretical $J-K'$, $M_{K'}$, colour-magnitude diagram (CMD) built for template stars (Ruelas-Mayorga 1991). We overplot the locations corresponding to the two XTE J1908+094 candidate counterparts, with the corresponding absolute magnitudes being computed for ten different values of the distance, ranging from 1 to 10 kpc, and dereddened for three different values of the hydrogen column density around the value of $N_H = 2.3 \times 10^{22}$ cm^{-2} measured by Woods et al. (2002).

Since each derived value of the absolute magnitude represents an upper limit, we can not accurately determine the distance of the source from the locations of their candidate counterparts on the CMD. However, the spectral type can be determined by the $J-K'$ colour, which is independent of the source distance. Therefore, according to the diagram, the companion star of object 1 would be an intermediate/late type main sequence star, probably of spectral type between A and K, and at a distance between 3 and 10 kpc. In the case of object 2, the companion star would be a late-type main sequence star, probably of spectral type later than K, and at a distance between 1 and 3 kpc.

The derived constraints on the spectral classification of the companion star are fully consistent with the non-

Date	MJD	Instrument	Object	J	H	K'
2002.04.25	52389.9	NTT/SOFI	Objects 1,2	$> 19.29 \pm 0.13$	$> 17.21 \pm 0.21$	$> 16.40 \pm 0.16$
2002.04.29	52393.9	NTT/SOFI	Objects 1,2	-	$> 17.39 \pm 0.16$	$> 16.52 \pm 0.16$
2002.06.17	52442.2	NTT/SOFI	Objects 1,2	$> 19.86 \pm 0.43$	$> 17.86 \pm 0.07$	$> 16.65 \pm 0.10$
2002.08.18	52504.3	CFHT/KIR	Object 1	20.14 ± 0.14	18.69 ± 0.04	17.77 ± 0.03
2002.08.18	52504.3	CFHT/KIR	Object 2	21.26 ± 0.35	18.98 ± 0.05	18.06 ± 0.04
2002.08.18	52504.3	CFHT/KIR	Objects 1+2	19.81 ± 0.37	18.07 ± 0.07	17.16 ± 0.05

Table 1. Photometry of the XTE J1908+094 candidate counterparts. The magnitudes in rows 1-3 were obtained with the SOFI instrument at the NTT and refer to the original candidate counterpart reported by Chaty et al. (2002a), which is actually a blend of two objects clearly resolved by the CFHT (objects 1 and 2, see Figure 1). Thus, the SOFI magnitudes have to be taken as upper limits on the magnitudes of both objects 1 and 2. The magnitudes in row 4-5 have been obtained with the KIR camera at the CFHT and refer to objects 1 and 2, respectively. Finally, the magnitudes in the last row represent the combined magnitudes of objects 1 and 2 (i.e. an artificial blending of CFHT objects) in order to compare it to the SOFI magnitudes.

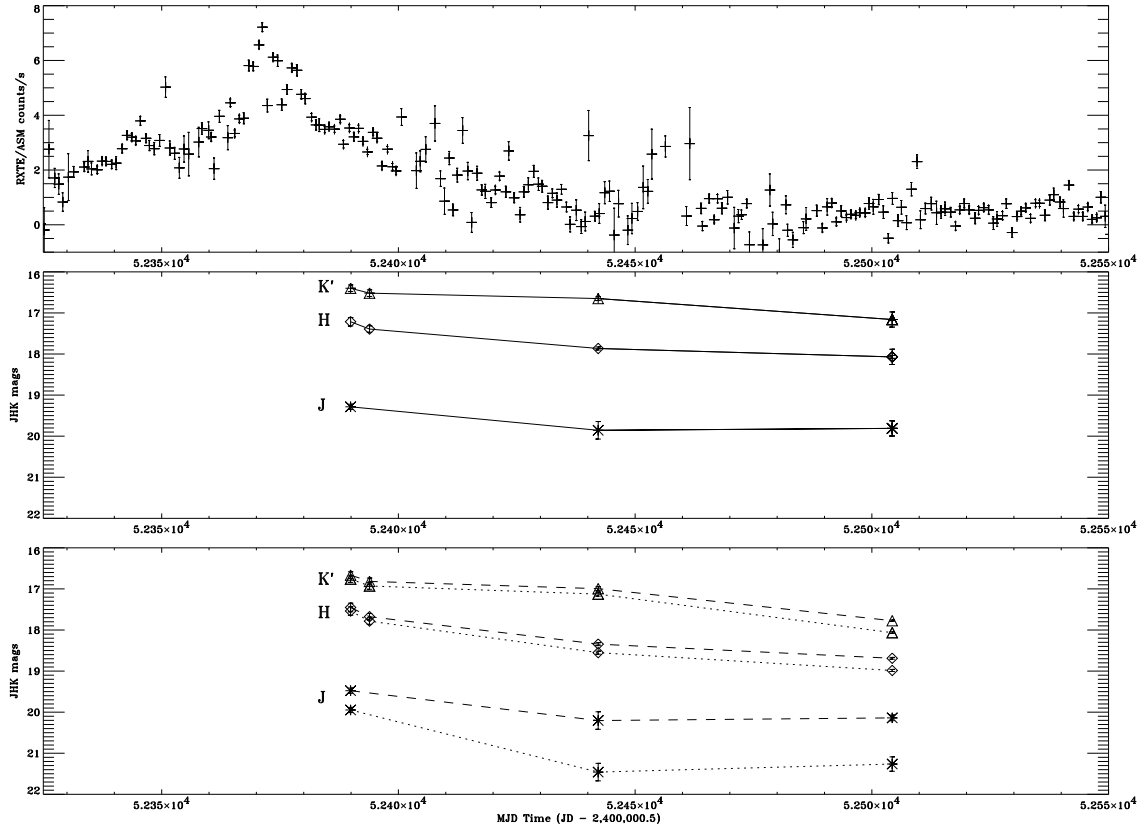

Figure 2. Multi-wavelength lightcurve of XTE J1908+094. Upper panel: *RXTE/ASM* $2-10$ keV lightcurve of XTE J1908+094. Flux values are in units of counts/s averaged over one day. Middle panel: observed IR lightcurves from the J ($*$), H ($\diamond$) and K' ($\triangle$) band magnitudes listed in Table 1. Per each passband, the points at the first three epochs are the magnitudes of the blend of objects 1 and 2 measured with the NTT/SOFI, while the points at the last epoch are the total magnitudes of objects 1 and 2 measured with the CFHT/KIR. Lower panel: Same as above, but the couple of points at the first three epochs are the estimated NTT/SOFI magnitudes for objects 1 and 2, corresponding to the difference between the total flux of the blend and the flux of object 2 and 1 (assumed constant), respectively. The couple of points at the last epoch are the measured CFHT/KIR magnitudes of objects 1 and 2. The dashed and dotted lines connect points associated to objects 1 and 2, respectively. The timescale is the same in the three panels, and the flux scale is the same in the middle and lower panels, for an easier comparison.

detection at $R \geqslant 23$ (Wagner & Starrfield 2002) and at $I \geqslant 22$ (Garnavich et al. 2002), since a K or M type star at a distance $\geqslant 1kpc$ would yield, for the expected absorption, $V \geqslant 30$. Near-infrared observations are therefore of prime importance to reveal highly absorbed sources.

However, taking into account the peak bolometric flux of XTE J1908+094, in't Zand et al. (2002b) have yielded a lower limit to the distance of 3 kpc (and even 6 kpc if the compact object is a black hole, with a minimum mass of 3 $M_{\odot}$). This makes it unlikely that object 2 is the actual

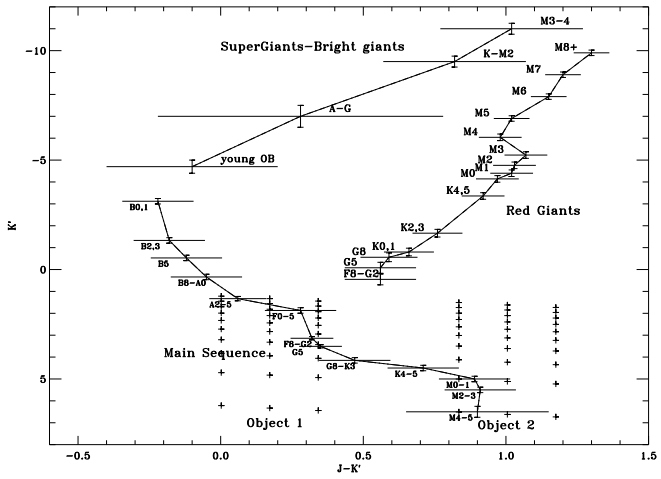

Figure 3. $J - K'$, $M_{K'}$,absolute CMD diagram computed for template main sequence stars (Ruelas-Mayorga 1991). The range of locations for the XTE J1908+094 companion star in the diagram has been derived from the absolute magnitudes of the two possible counterparts, computed taking the minimum apparent magnitudes on 2002 August 18th, and assuming that all the flux is produced from the companion star. Three different values of the interstellar extinction have been applied i.e. $A_V = 11.19, 12.9, 13.9$ magnitudes from right to left, respectively. $A_V = 12.9$ magnitudes corresponds to a column density $N_H = 2.3 \times 10^{22}$ (Woods et al. 2002), using the relation from Predehl & Schmitt (1995). From bottom to top the crosses correspond to a source distance increasing from 1 to 10 kpc. According to the diagram, in the case of object 1, the companion star would be be an intermediate/late type main sequence star of spectral type between A and K, located between 3 and 10 kpc. In the case of object 2, the companion star would be a late-type main sequence star of spectral type later than K, located between 1 and 3 kpc.

counterpart of XTE J1908+094. Therefore, our analysis of the CMD favours, as does the astrometry, object 1 as the most likely counterpart.

4 CONCLUSION

We have reported on CFHT adaptive optics observations of the black hole candidate XTE J1908+094 which showed that the previously reported counterpart (Chaty et al. 2002a) was in fact a blend of two objects. A new and more accurate astrometric analysis provides qualitative evidence that the brighter of the two (called object 1) is a more likely counterpart. Accurate photometry performed on four sets of observations spanning 4 months have shown a decrease of the NIR flux for one (or both) of the two candidates, consistent with the X-ray decay, showing that one of the two is almost certainly the real counterpart of XTE J1908+094. After dereddening and assuming that the flux represents upper limits to the contribution of the companion star, we derived that the companion star could be i) either an intermediate/late type main sequence star of spectral type between A and K, located between 3 and 10 kpc, or ii) a late-type main sequence star of spectral type later than K, located between 1 and 3 kpc. However, since a lower limit to the distance of 3 kpc has been derived from the peak bolometric flux of XTE J1908+094 by in't Zand et al. (2002b), both colors and magnitudes, as well as the astrometry, would rule out object 2 and favour object 1 as the most likely counterpart of the X-ray source.

Further near-infrared observations are needed, especially during the next outburst of the source, in order to monitor the variability of both candidate counterparts and eventually confirm (or not) our identification of object 1 as the counterpart of XTE J1908+094. Getting some spectroscopy, although difficult because of faint and blended candidates, should be feasible with next generation instruments, and would finally better constrain both the spectral type and distance of the companion star.

5 ACKNOWLEDGEMENTS

This work is partially supported through Agenzia Spaziale Italiana (ASI), Ministero dell'Istruzione, Università e Ricerca Scientifica e Tecnologica (MIUR – COFIN), and Istituto Nazionale di Astrofisica (INAF) grants. This research has made use of NASA's Astrophysics Data System. Bibliographic Services and quick-look results provided by the ASM/RXTE team.

REFERENCES

Casali 1992, UKIRT Newsletter, 4, 33
Chaty S., Mignani R. P., Israel G. L., 2002a, Mon. Not. R. astr. Soc., 337, L23
Chaty S., Mignani R. P., Vanzi L., 2002b, IAU Circ., 7897, 2+
Feroci M., Reboa L., 2002, IAU Circ., 7861, 2+
Garnavich P., Quinn J., Callanan P., 2002, IAU Circ., 7877, 4
in 't Zand J. J. M., Capalbi M., Perri M., 2002a, IAU Circ., 7873, 1+
in't Zand J. J. M., Miller J. M., Oosterbroek T., Parmar A. N., 2002b, Astron. Astrophys., 394, 553
Massey P., Davis L., 1992, A User's Guide to Stellar CCD Photometry with IRAF
Predehl P., Schmitt J.H.M.M., 1995, A&A, 293, 889
Ruelas-Mayorga R. A., 1991, Revista Mexicana de Astronomia y Astrofisica, 22, 27
Rupen M. P., Dhawan V., Mioduszewski A. J., 2002, IAU Circ., 7874, 1+
Wagner R. M., Starrfield S., 2002, The Astronomer's Telegram, #86, 86, 1+
Woods P. M., Kouveliotou C., Finger M. H., Gogus E., Swank J., Markwardt C., Strohmayer T., 2002, IAU Circ., 7856, 1